Published in "Phosphorus, Sulfur, and Silicon and the Related Elements 193(4): 257-266, 2017" which should be cited to refer to this work.

The synergistic cooperation of NH···O and CH···O hydrogen bonds in the structures of three new phosphoric triamides

Anahid Saneei[a], Mehrdad Pourayoubi[a], Jerry P. Jasinski[b], Titus A. Jenny[c], Aurelien Crochet[d], Katharina M. Fromm[d], and Amanda C. Keeley[b]

[a]Department of Chemistry, Faculty of Science, Ferdowsi University of Mashhad, Mashhad, Iran; [b]Department of Chemistry, Keene State College, Keene, NH, USA; [c]Department of Chemistry, University of Fribourg, Rte du Musée 9, Fribourg, Switzerland; [d]Fribourg Centre for Nanomaterial's, FriMat, University of Fribourg, Chemin du Musée 3, Fribourg, Switzerland

ABSTRACT

The supramolecular assemblies of three new phosphoric triamides, $\{(C_6H_5CH_2)(CH_3)N\}_2(4\text{-}CH_3\text{-}C_6H_4C(O)NH)P(O)$ (**1**), $\{(C_6H_{11})(CH_3)N\}_2(4\text{-}CH_3\text{-}C_6H_4C(O)NH)P(O)$ (**2**) and $\{(C_2H_5)_2N\}_2(4\text{-}CH_3\text{-}C_6H_4C(O)NH)P(O)$ (**3**) were studied by single crystal X-ray diffraction as well as by Hirshfeld surface analysis. It was found that a synergistic cooperation of NH···O and CH···O hydrogen bonds occurs in all three structures, but forming unique supramolecular architectures individually. Along with the presence of centrosymmetric dimers in **1, 2** and **3**, based on a classical NH···O hydrogen bond, the presence of weak CH···O interactions play an additional and vital role in crystal architecture and construction of the final assemblies, collectively identified as a centrosymmetric dimer (0D), a 1-D array and a 3-D network, respectively. These differences in superstructures are related to the effect of aromatic, bulk and flexible groups used in the molecules designed, with a similar C(O)NHP(O) backbone. The NH···O contacts in **1, 2** and **3** are of the "resonance-assisted hydrogen bond" types and also the *anti*-cooperativity effect can be considered in the multi-acceptor sites P═O in **1** and **2** and C═O in **3**. All three compounds were further studied by 1D NMR experiments, 2D NMR techniques (HMQC and HMBC (H–C correlation)), high resolution ESI–MS, EI–MS spectrometry and IR spectroscopy methods.

KEYWORDS

Phosphoric triamide; hydrogen bond; supramolecular assembly; Hirshfeld surface analysis; 2D NMR spectroscopy

GRAPHICAL ABSTRACT

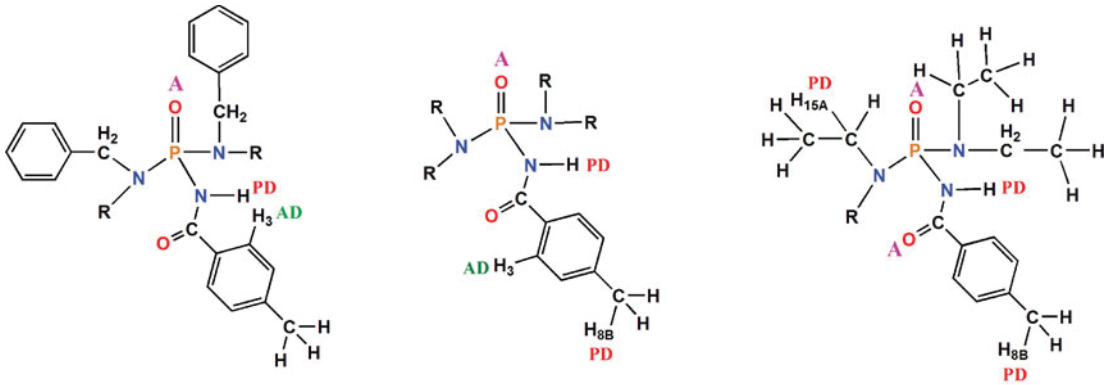

(1) (2) (3)

Introduction

Crystal engineering is considered as a design engine for new materials with predefined properties, which has emerged as a major research area during the past decade due to its tremendous and diverse applications.[1,2] Currently, it is recognized as a multidisciplinary area owing to its implications in material chemistry, supramolecular chemistry, molecular recognition and biology.[3,4] The analytical component of crystal engineering consists of studies of various non-covalent interactions that are responsible for crystal assembly.[5,6]

Among the various non-covalent interactions, hydrogen bonding is the most studied owing to its existence in many

CONTACT Mehrdad Pourayoubi pourayoubi@um.ac.ir Department of Chemistry, Faculty of Science, Ferdowsi University of Mashhad, Mashhad, 91779, Iran.

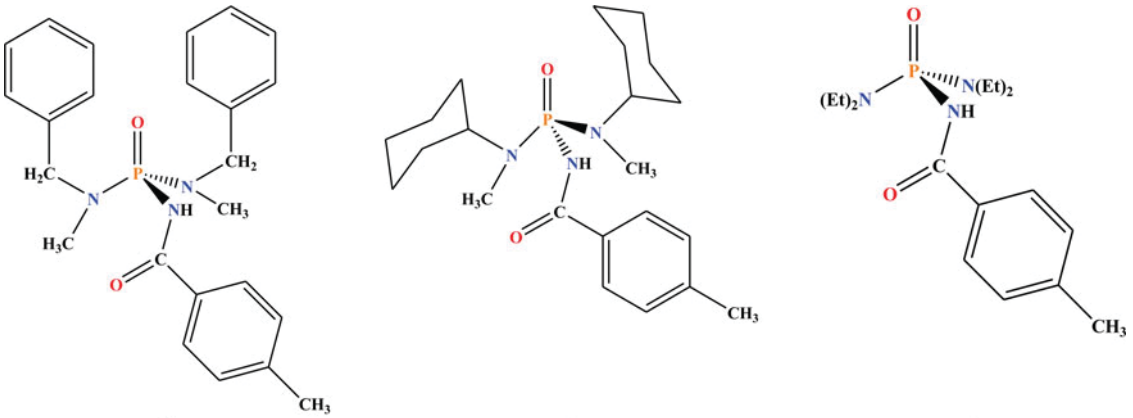

1 **2** **3**

Figure 1. Chemical structures of **1**–**3**.

biological systems.[7] It is well established that strong and moderate hydrogen bonds such as OH···O, NH···O and OH···N have extensively influenced the properties of molecular crystals and also have important roles in supramolecular assemblies and crystal architectures.[8–10] On the other hand, although it is long known that numerous weaker intermolecular hydrogen bond types occur in a vast variety of chemical and biological systems, perhaps they are considered with lower degrees of importance in directing supramolecular assemblies.[11] However, crystal packing is not simply determined by a small number of strong interactions, but by the cooperation and competition of a large number of strong and weak intermolecular interactions.[12,13] Moreover, it is found that many properties of some interconnected hydrogen bonds in a crystal are not just the sum of those of constituting isolated bonds. These hydrogen bonds may enhance or reduce the strengths of each other, through mechanisms as examined *via* cooperativity or *anti*-cooperativity concepts.[14]

The weak hydrogen bonds based on C–H donors are important both as secondary and, in fewer cases, as primary interactions in determining crystal structures, in the stabilization of inclusion complexes and in recognition processes.[13,15] From various weak CH···X (X = O, N, Cl, π and so on) hydrogen bonding interactions, investigation has been especially concentrated on the CH···O interactions[16,17] and such interactions are the best known of all weak hydrogen bond types. That is why several reviews have described these developments and also the historical background of the research on CH···O hydrogen bonds in the fields of general structural chemistry[18] and of structural biology.[19]

Organophosphorous compounds such as phosphoramides have a highly polarized P═O group that facilitates the formation of hydrogen bonds. In addition to the interaction of a phosphoryl group with O–H and N–H functional groups, which usually forms strong or moderate hydrogen bonds, this group is also capable of forming hydrogen bonds with relatively low acidic hydrogen atoms such as in CH···OP.[20] It seems that although this type of interaction is weak, it plays an important role in crystal packing. From this viewpoint, phosphoramides may be interesting compounds in the area of crystal engineering, not only for nearly strong NH···OP hydrogen bonds, but also for a large number of weak contacts that exist in their structures.[21,22]

Considering the importance of weak hydrogen bonds in determining the architecture of supramolecular assemblies of phosphoryl compounds, we have synthesized three new compounds belonging to the phosphoric triamide family with a similar C(O)NHP(O) backbone and similar *p*-CH_3-C_6H_4 substituent attached to the C═O group, but with different substituents attached to the P═O group. The chemical structures of these molecules are presented in Figure 1. The three molecules designed all include only one N–H unit, capable for the formation of strong hydrogen bonds. Differences in the substituents are related to the presence of aromatic, bulk or flexible groups bonded to phosphorus. The cooperation/competition between P═O and C═O groups as acceptors and NH and CH as donors have been examined. Thus, we have investigated the role and influence of hydrogen bonds formed in the molecular architecture and supramolecular assembly by X-ray crystallography combined with 3D-Hirshfeld surface maps and 2D-fingerprint plots. The newly synthesized compounds have also been studied by ^{1}H, ^{13}C, ^{31}P, ^{1}H–^{13}C HMQC and ^{1}H–^{13}C HMBC NMR, ESI–MS and EI–MS spectrometry and IR spectroscopy methods.

Results and discussion

X-ray crystallography investigation

Structural features

Compounds **1**–**3** crystallize in the monoclinic crystal system, within the $P2_1/n$ space group for **1** and **2** and the $P2_1/c$ space group for **3**. The crystallographic data and refinement parameters are presented in Table 1. The asymmetric units of all three compounds contain one complete molecule (Figures 2–4). The bond angles at the P atoms are in the range of 104.04(7)° (N2-P1-N3) to 118.78(7)° (O1-P1-N3) for **1**, 105.25(7)° (N2-P1-N3) to 116.79(8)° (O2-P1-N3) for **2** and 105.66(9)° (O2-P1-N1) to 115.58(10)° (O2-P1-N2) for **3**. These angles are in agreement with a distorted tetrahedral configuration with calculated $\tau 4$ geometry index values[23] of 0.91 for **1** and 0.94 for **2** and **3** (in comparison with the $\tau 4 = 1$ for ideal tetrahedral).

The P═O bond lengths in **1, 2** and **3** are within the standard values of analogous structures[24,25] *i.e.* 1.4794(11) Å for **1**, 1.4828(12) Å for **2** and 1.4855(16) Å for **3**. The P–N bond lengths

Table 1. Crystal data and structure refinement for compounds **1**–**3**.

	Compound 1	Compound 2	Compound 3
Empirical formula	$C_{24}H_{28}N_3O_2P$	$C_{22}H_{36}N_3O_2P$	$C_{16}H_{28}N_3O_2P$
Formula weight	421.46	405.51	325.38
Temperature (K)	173(2)	173(2)	200(2)
Wavelength (Å)	1.54184	1.54184	1.54186
Crystal system	Monoclinic	Monoclinic	Monoclinic
Space group	$P2_1/n$	$P2_1/n$	$P2_1/c$
a (Å)	8.8301(6)	14.0673(3)	11.4978(10)
b (Å)	13.1198(7)	10.6709(3)	13.4479(11)
c (Å)	19.4513(10)	15.1367(4)	11.8421(10)
β (°)	94.540(5)	90.952(2)	92.799(7)
V (Å^3)	2246.3(2)	2271.87(9)	1828.9(3)
Z	4	4	4
Density (calculated) (g/cm^3)	1.246	1.186	1.182
Absorption coefficient (mm^{-1})	1.279	1.234	1.414
F(000)	896	880	704
Index ranges	$-10 \le h \le 10, -16 \le k \le 14, -23 \le l \le 18$	$-17 \le h \le 11, -13 \le k \le 12, -18 \le l \le 18$	$-13 \le h \le 13, -16 \le k \le 16, -13 \le l \le 13$
Reflections collected	14000	14064	13272
Independent reflections	4394 [$R_{(int)} = 0.0488$]	4463 [$R_{(int)} = 0.0390$]	3066 [$R_{(int)} = 0.0726$]
Refinement method	Full-matrix least-squares on F^2	Full-matrix least-squares on F^2	Full-matrix least-squares on F^2
Data/restraints/parameters	4394/0/275	4463/0/257	3066/0/205
Goodness-of-fit on F^2	1.042	1.053	1.199
Final R indices [$I > 2\sigma(I)$]	$R_1 = 0.0442$, $wR_2 = 0.1221$	$R_1 = 0.0433$, $wR_2 = 0.1167$	$R_1 = 0.0671$, $wR_2 = 0.1891$
R indices (all data)	$R_1 = 0.0496$, $wR_2 = 0.1280$	$R_1 = 0.0517$, $wR_2 = 0.1237$	$R_1 = 0.0693$, $wR_2 = 0.1915$
Largest diff. peak and hole (e.Å^{-3})	0.399 and −0.478	0.411 and −0.330	1.015 and −0.505

are typical of those found in these compounds and shorter than a typical phosphorus-nitrogen single bond (1.77 Å)[26] due to a further interaction of the nitrogen atom with the phosphoryl group, besides the σ-bond. In all three structures, the O=P–N_{CP} angles are contracted more than the two normal O=P–N_P angles, Table 2 (in our discussion, N_{CP} is the nitrogen atom in the C(O)NHP(O) segment and N_P shows two other nitrogen atoms bonded to the phosphorus atom). The N atoms bonded to the P=O group in the three structures all show small deviations from planar configurations, with the largest deviation being observed for the N3 atom of **1**. Here the bond-angle sum at the N atom is about 8° less than the ideal sp^2 bond-angle sum of 360°.

Supramolecular assembly mediated by NH···O and CH···O hydrogen bonds

In the structure **1**, the molecules are linked through pairs of N_{CP}–H···OP hydrogen bonds, forming centrosymmetric dimers with an $R_2^2(8)$ graph-set ring motif (Figure 5, Table 3). Furthermore, the O1(P) atom takes part in a weak intermolecular C3-H3···O1 interaction and the ring motif formed, $R_2^1(7)$, is fused to the primary dimer motif and does not extend the dimensionality of network. The oxygen atom of the carbonyl group is only involved in a low-angle intramolecular C16-H16A···O2 hydrogen bond, forming an $S_1^1(7)$ graph-set motif.

By considering only classical hydrogen bonds, structures **2** and **3** also include centrosymmetric dimers with $R_2^2(8)$ graph-set

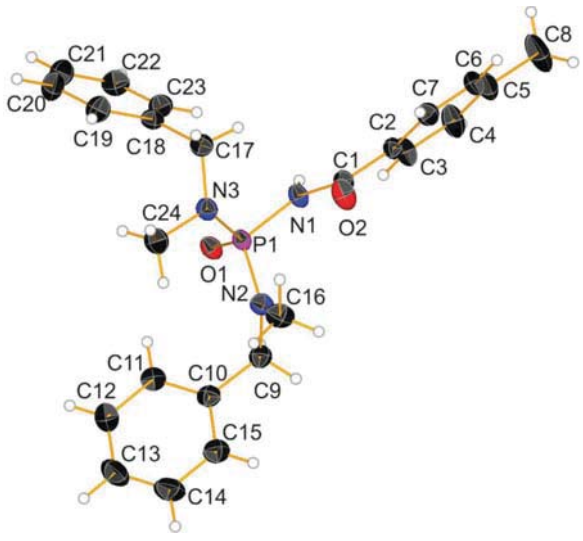

Figure 2. Displacement ellipsoid plot (50% probability) is shown for **1** with the atom numbering scheme. H atoms are drawn as spheres of arbitrary radii.

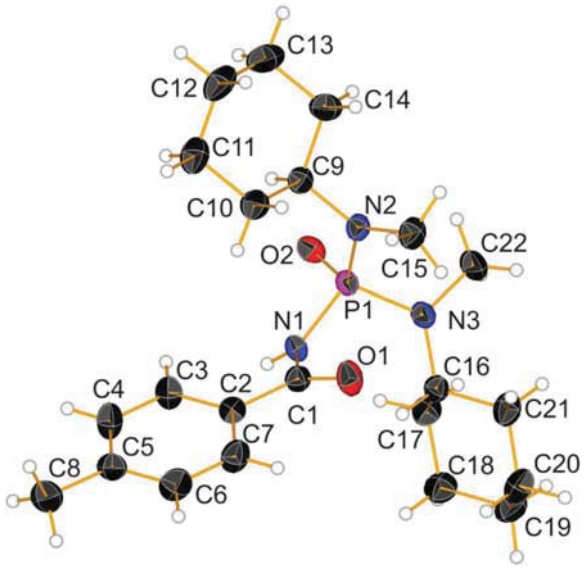

Figure 3. Displacement ellipsoid plot (50% probability) is shown for **2** with the atom numbering scheme. H atoms are drawn as spheres of arbitrary radii.

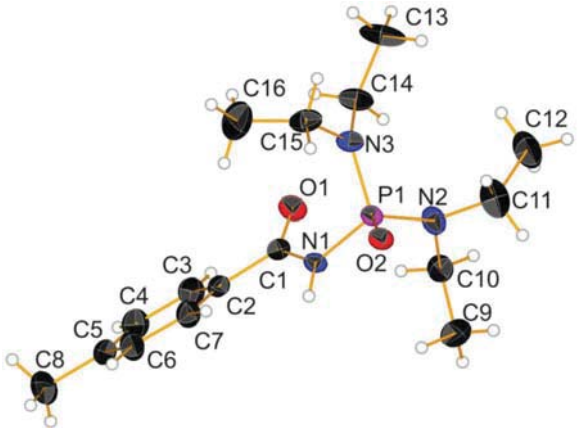

Figure 4. Displacement ellipsoid plot (50% probability) is shown for **3** with the atom numbering scheme. H atoms are drawn as spheres of arbitrary radii.

Table 2. Selected bond distances (Å) and angles (°) for compounds **1**–**3**.

Compound **1**			
P1-O1	1.4794(11)	N1-C1	1.3708(19)
P1-N1	1.6808(13)	N2-C9	1.470(2)
P1-N2	1.6380(14)	N2-C16	1.459(2)
P1-N3	1.6449(14)	N3-C17	1.476(2)
O2-C1	1.2224(19)	N3-C24	1.465(2)
O1-P1-N1	105.68(6)	N1-P1-N3	105.50(7)
O1-P1-N2	110.04(7)	N2-P1-N3	104.04(7)
O1-P1-N3	118.78(7)	C1-N1-P1	127.89(11)
N1-P1-N2	112.95(7)		
Compound **2**			
P1-O2	1.4828(12)	N1-C1	1.376(2)
P1-N1	1.6784(13)	N2-C9	1.475(2)
P1-N2	1.6409(13)	N2-C15	1.467(2)
P1-N3	1.6350(14)	N3-C16	1.474(2)
O1-C1	1.2185(19)	N3-C22	1.473(2)
O2-P1-N1	106.26(6)	N1-P1-N3	107.67(7)
O2-P1-N2	110.36(7)	N2-P1-N3	105.25(7)
O2-P1-N3	116.79(8)	C1-N1-P1	125.49(11)
N1-P1-N2	110.48(7)		
Compound **3**			
P1-O2	1.4855(16)	N1-C1	1.373(3)
P1-N1	1.6874(18)	N2-C10	1.470(3)
P1-N2	1.634(2)	N2-C11	1.499(4)
P1-N3	1.6380(19)	N3-C14	1.467(3)
O1-C1	1.221(3)	N3-C15	1.475(3)
O2-P1-N1	105.66(9)	N1-P1-N3	111.20(10)
O2-P1-N2	115.58(10)	N2-P1-N3	106.56(10)
O2-P1-N3	110.49(9)	C1-N1-P1	126.54(15)
N1-P1-N2	107.36(10)		

Table 3. Hydrogen bonds geometries for compounds **1**–**3**.

D–H···A	d(D–H)	d(H···A)	d(D···A)	∠(DHA)	Symmetry code
1					
N1-H1···O1^{i}	0.86	1.99	2.8406(16)	167	(i) $-x+2, -y+2, -z+1$
C9-H9B···O1	0.97	2.46	2.807(2)	108	
C3-H3···O1^{i}	0.93	2.58	3.174(2)	122	(i) $-x+2, -y+2, -z+1$
C16-H16A···O2	0.96	2.56	3.138(2)	119	
2					
N1-H1···O2^{i}	0.86	1.95	2.7947(17)	168	(i) $-x+1, -y+1, -z$
C8-H8B···O2^{ii}	0.96	2.54	3.480(2)	165	(ii) $x, -1+y, z$
C9-H9···O2	0.98	2.43	2.9797(19)	115	
C3-H3···O2^{i}	0.93	2.58	3.234(2)	129	(i) $-x+1, -y+1, -z$
3					
N1-H1···O2^{i}	0.82	1.98	2.790(2)	167	(i) $-x+1, -y, -z+1$
C15-H15A···O1^{ii}	0.97	2.60	3.544(3)	166	(ii) $x, -y+1/2, z+1/2$
C8-H8B···O1^{iii}	0.96	2.40	3.329(2)	163	(iii) $-x, -1/2+y, 1/2-z$

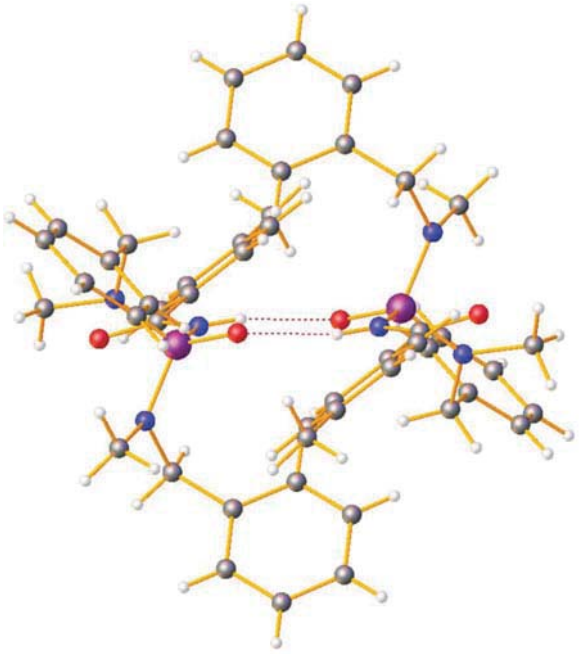

Figure 5. A view of crystal packing in structure **1** is given, showing the hydrogen-bonded dimer formed through two N_{CP}—H …O═P hydrogen bonds. The hydrogen bonds are shown as dashed lines.

ring motifs formed *via* pairs of N_{CP}–H···OP hydrogen bonds, similar to one what was reported for structure **1** (Figures 6 and 7, respectively); but the weak CH···O interactions are the main key differences in the final patterns and types of hydrogen bond networks displayed among the three structures. In structure **2**, similar to **1**, only the oxygen atom of the phosphoryl (O2) group cooperates in the crystal packing based on intermolecular hydrogen bonds. Thus, the hydrogen-bonded dimers further interplay through C8-H8B···O2 and C3-H3···O2 weak

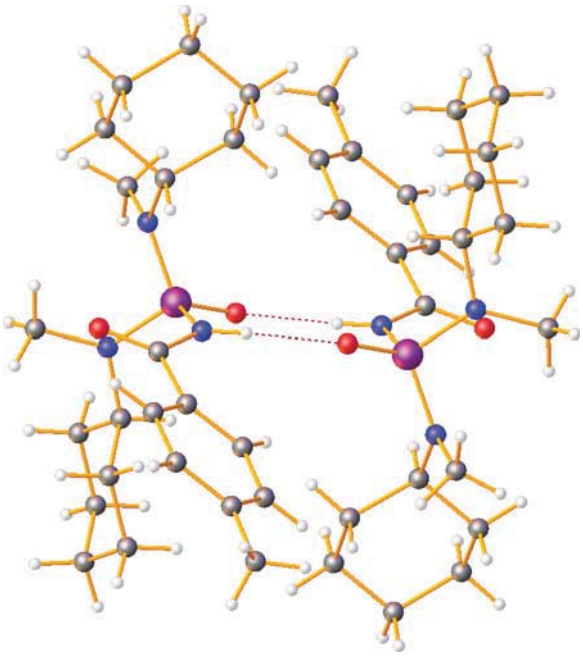

Figure 6. A view of crystal packing in structure **2** is given, showing the hydrogen-bonded dimer formed through two N_{CP}—H …O═P hydrogen bonds. The hydrogen bonds are shown as dashed lines.

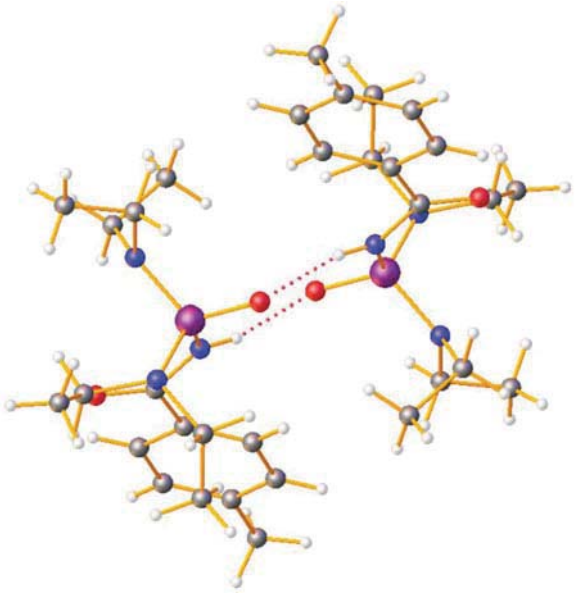

Figure 7. A view of crystal packing in structure **3** is given, showing the hydrogen-bonded dimer formed through two N_{CP}—H …O═P hydrogen bonds. The hydrogen bonds are shown as dashed lines.

interactions in a 1D array along the *b* axis (Figure 8), including $R_2^1(7)$ and $R_4^2(14)$ hydrogen-bonded ring motifs. The former motif is constructed from one CH (C3-H3) and one NH as donor groups, while the latter motif is constructed from pairs of both CH donors noted (C8-H8B and C3-H3), with the phosphoryl group as the acceptor for both of the two motifs. On the other hand, the three cyclic hydrogen-bonded motifs noted are fused to each other and participate with the oxygen atom of the phosphoryl group, which acts as a triple acceptor in an (N1-H1···)(C3-H3···)(C8-H8B···)OP grouping. When considering the intramolecular C9-H9···O2 hydrogen bond in **2**, an $S_1^1(5)$ graph-set motif is also formed, and hence it can be stated that the phosphoryl group behaves as a fourfold acceptor in this structure. This hydrogen-bonded motif consists of five different atoms.

The oxygen atom of the carbonyl group does not take part in intermolecular hydrogen bonding. This is due to the bulk $N(CH_3)(C_6H_{11})$ group which surrounds the C═O group and takes it out by accessing it as an acceptor amongst the intermolecular hydrogen bonds. The crowded activity that arises from this bulk group also leads to a novel near H···H contact which will be discussed in the Hirshfeld surface analysis.

In the crystal structure of **3**, against to the structures **1** and **2**, the oxygen atom of the carbonyl group participates in weak CH···O hydrogen bond activity. In this structure, the dimer motifs formed through N_{CP}–H···O═P hydrogen bonds ($R_2^2(8)$) are further connected through CH···O hydrogen bonds to form a 3D network (Figure 9). This superstructure includes $R_4^4(30)$ and $R_4^2(26)$ ring motifs which are both built from C8-H8B···O1-C1 and C15-H15A···O1-C1 hydrogen bonds, whereby the C═O group acts as a double hydrogen-bond acceptor and the two CH units are related to the methyl group attached to the phenylene ring and to the CH_2 of the flexible $(CH_3CH_2)_2N$ fragment.

The NH unit of the C(O)NHP(O) backbone in all three phosphoric triamide structures (**1, 2** and **3**) takes part in the hydrogen bond so-called as "resonance-assisted". Typical for such a mechanism is the case that an amide N–H group becomes a stronger donor if the amide O atom accepts a hydrogen bond, *D*–H···O═C–N–H.[14] For **1, 2** and **3**, this polarization occurs as the P═O and/or C═O group becomes involved in a CH···O hydrogen bond. As it is well-known, the resonance-assisted hydrogen bond or "π-bond cooperativity" enhances the strength of hydrogen bond involved.

Hydrogen bonds may not only enhance, but also reduce the strengths of each other. For a double-acceptor atom, a previous article has demonstrated that two roughly parallel donor dipoles repel each other, which leads it to reduce the strength of each hydrogen bond by the other in a three-centred $(D^1—H···)(D^2—H···)A$ grouping (D^1 and D^2 = donors and A = acceptor). This is the so-called *anti*-cooperativity effect. Structures **1, 2** and **3** also include multi-centred oxygen atoms, as discussed earlier. The cooperativity and *anti*-cooperativity mechanisms are responsible for the non-additivity of hydrogen bond energies.[14]

In summary, the CO group of both structures **1** and **2** does not form access to the intermolecular hydrogen bond, while the PO group takes part in a multi-centred hydrogen bond grouping. In these two structures, the supramolecular assembly was mediated by NH···O and CH···O hydrogen bonds, but the resulting hydrogen bond patterns are a centrosymmetric dimer (0D) for **1** and a 1D array for **2**. The CH···O in structure **1** is

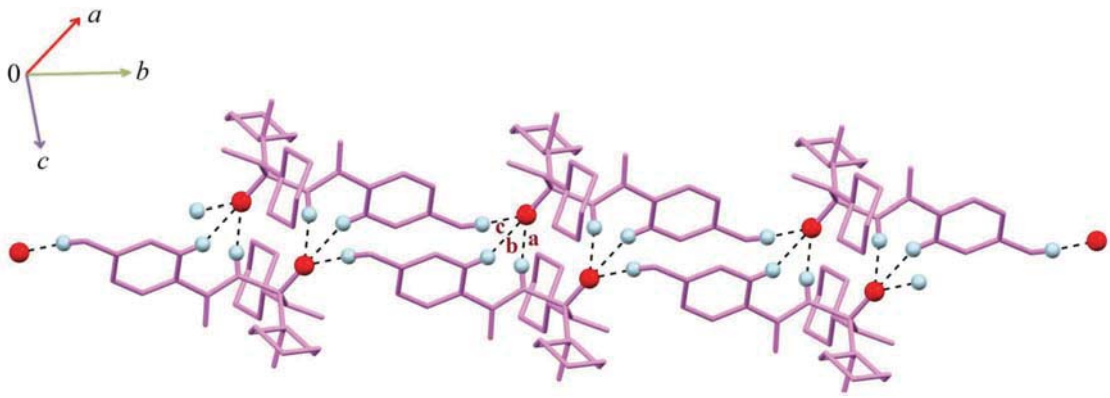

Figure 8. A view of 1D arrangement of structure **2** along the *b* axis which is formed by connection of the adjacent dimers, the labels "**a**", "**b**" and "**c**" near to dashed lines denote N1-H1···O2, C3-H3···O2 and C8-H8B···O2 hydrogen bonds, respectively.

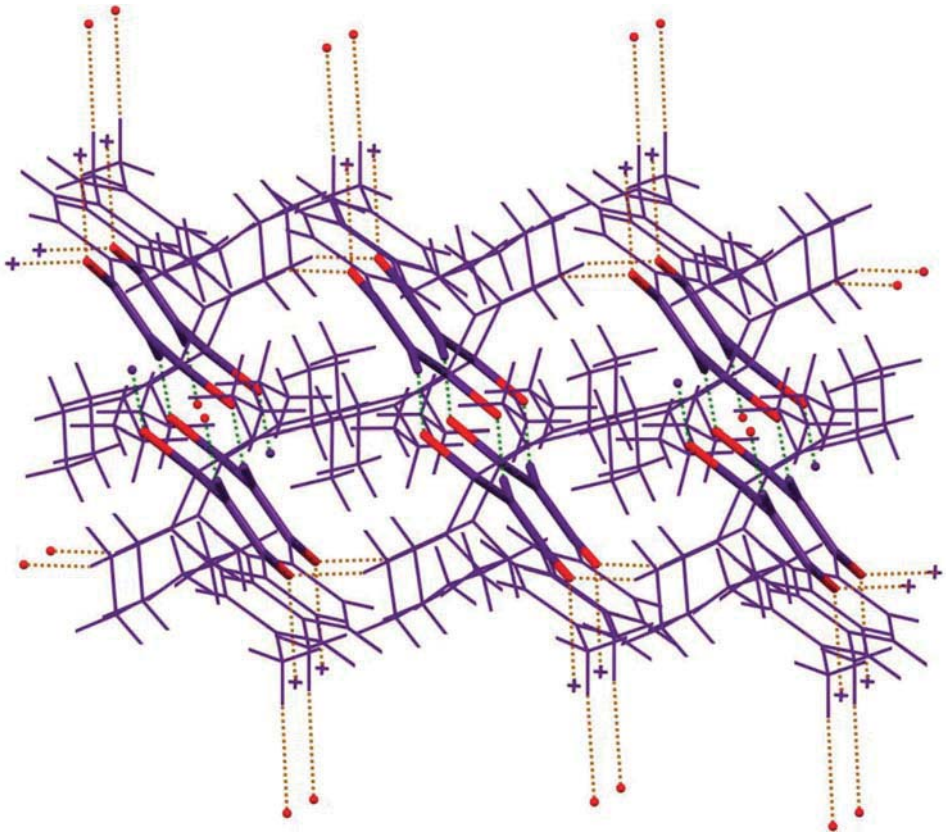

Figure 9. A view of 3D network of structure **3** which is formed by connection of adjacent dimers through C8-H8B···O1 and C15-H15A···O1 weak interactions (brown dashed lines in the electronic version of paper). The green dashed lines indicate the N_{CP}—H …O═P hydrogen bonds.

an auxiliary hydrogen bond with an NH···O interaction in the dimer formed and does not extend the dimensionality.

In **3**, the PO group takes part in the normal hydrogen bond and the CO group cooperates in weak hydrogen bonding. The cooperation of NH···O and CH···O hydrogen bonds leads to a 3D superstructure. The donor and acceptor sites in the three crystal structures are pictorially represented in Figure 10. The differences in the hydrogen bond patterns and the numbers and types of donor/acceptor sites involving in hydrogen bonding interactions are reflected in the types and percentages of interactions and will be discussed in the section on Hirshfeld surface analysis and fingerprint plots.

Hirshfeld surface analysis

A background of the Hirshfeld surface analysis and fingerprint plots[27–31] and the details of such analysis for structures **1, 2** and **3** are provided in the Supplemental Materials. In a Hirshfeld map, red color areas denote to the contacts shorter than vdW radii. Within such contacts, shorter and stronger ones are associated with large and deep red spots, while the longer and weaker show up as smaller and lighter red spots on the surface. The highlighted sections about Hirshfeld surfaces are the deep red color region for NH···O contacts and the lighter red areas for CH···O contacts in all three structures (Figure S1).

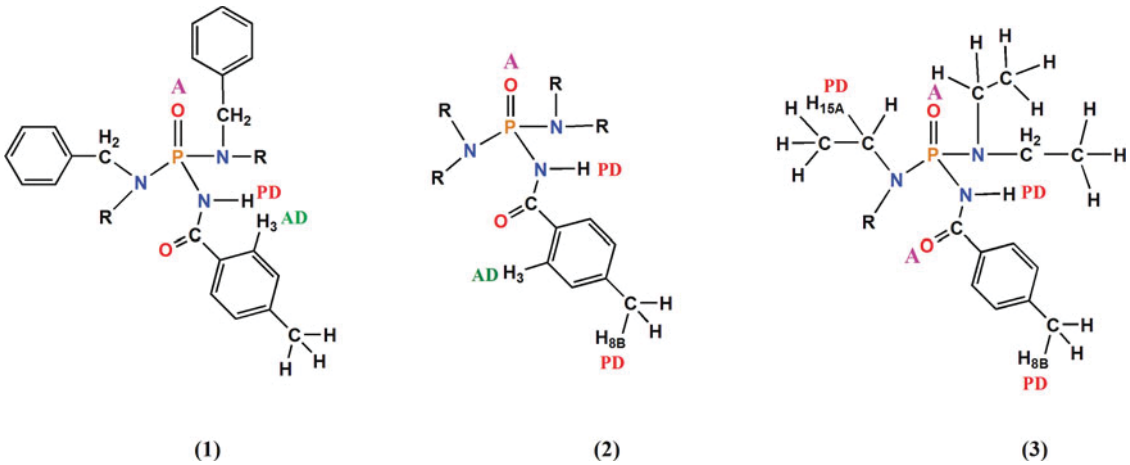

Figure 10. The acceptor and donor sites in **1**–**3**, taking part in intermolecular hydrogen bonding, are specified. The label "PD" denotes the donor site responsible for the dimensionality (principal donor) and the label "AD" denotes the auxiliary donor which exists along with a principal donor in a multi-centered hydrogen bond grouping.

Furthermore, structure **1**, with the most unsaturated systems with respect to two other structures, reveals weak C···H contacts and structure **2** with higher number of hydrogen atoms and the bulk $N(CH_3)(C_6H_{11})$ groups shows an H···H contact. Both types of interactions noted are seen as very pale red regions in the corresponding Hirshfeld surface maps, as shown in Figure S1 (Supplemental Materials).

A fingerprint plot is depicted on an *XY*-grid formed by d_e, d_i pairs ($X = d_i$ and $Y = d_e$) and d_e and d_i are described as distances from a point on the Hirshfeld surface to the nearest nucleus outside and inside the surface, respectively. The full fingerprint plots of all three structures (Figure S2) include two sharp spikes which are related to the strong interactions (O···H), with the minimum $d_i + d_e$ values for the closest contact. A survey of full plots for **1**–**3** shows that upper d_e and d_i values on the full FP of **3** are more compact than those in the full FPs of **1** and **2** (d_e < 2.7 Å and d_i < 2.7 Å in both **1** and **2** and d_e < 2.5 Å and d_i < 2.5 Å in **3**), which indicates more efficient packing in **3**. Moreover, the divided fingerprint plots which are presented in Figures S3–S5 reveal that the H···H interactions have the most contribution portions with respect to the other contacts in all structures (Figures S3a–S5a). The maximum O···H contacts are found for structure **3** (Figure S5b) with more efficient packing, while the maximum C···H contacts are observed for structure **1** (Figure S3c) which has the highest numbers of unsaturated C atoms.

Spectral studies

A high resolution ESI–MS characterization was carried out for compounds **1**–**3**, which supports the observed structures. The EI mass spectra of compounds **1**–**3** were also recorded which show molecular ion peaks $[M]^+$ at m/z 421, 405 and 325, respectively. All three compounds show $[M–1]^+$ fragment peaks, which can be attributed to loss of an H atom. The peak at m/z 117 in the mass spectra of all three compounds is assigned to the 4-methylphenylcyanide radical-cation which formed by removal of amidophosphoric acid from the parent ion, as was reported for $[C_6H_5C(O)NH]P(O)[OR]_2$ phosphoramides by removing of an ester of phosphoric acid.[32] The observation of this fragment indicates that the parent radical-cation rapidly undergoes a migration of phosphorus from nitrogen to oxygen. From this resulting isomer, a McLafferty fragmentation would produce the $C_8H_7N^+$ radical-cation plus neutral amidophosphoric acid. Typical for a McLafferty fragmentation is the fact that the charge could appear alternatively on either fragment, *i.e.* also the amidophosphoric acid part could be charged and hence may be observed. However, the pathway involving elimination of an amidophosphoric acid molecule is preferred, due to the absence of an amidophosphoric acid radical-cation in the mass spectra of compounds **1**–**3**. The base peak for **1** is observed at m/z 119, which is evidence for a bond scission of the amide bond in the NH-C(O) section generating the CH_3-$C_6H_4C(O)^+$ fragment, as reported for analogous compounds.[33] This fragment is also prominent in compounds **2** and **3** (more than 65%). For compounds **2** and **3** the base peaks are revealed at m/z = 112 and 28 which are attributed to the $N(CH_3)(C_6H_{11})^+$ and $C_2H_4^+$ fragment ions, respectively.

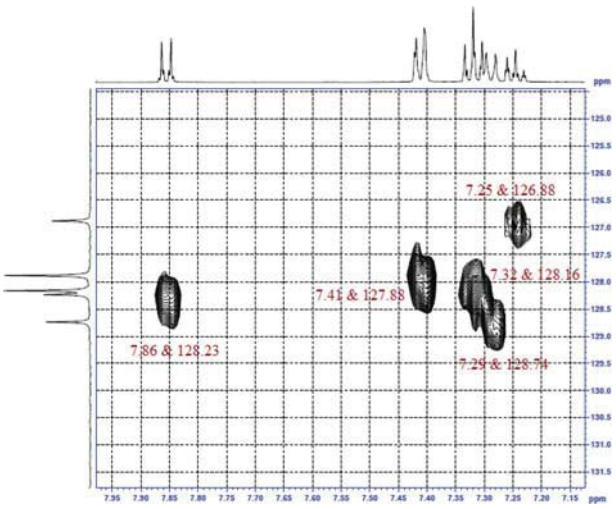

Figure 11. One bond C–H correlation in the HMQC spectrum of **1** showing only the aromatic parts.

Detailed explanations of IR, and 1D NMR spectra (Figures S6–S14) including assignments are reported in the Supplemental Materials. The 2D ^1H–^{13}C HMQC spectra of compounds **1**–**3** provide information on the interactions between the protons and the carbon atoms, which are directly attached to each other (Table 4). As a representative, the following discussion is based on the spectrum for compound **1** (Figure 11). It can be deduced from Figure 11 that H2 and H6 at δ = 7.86 ppm in a tolyl part are correlated with C2 and C6 at δ = 128.23 ppm. This one-bond ^1H–^{13}C spectrum also indicates the correlation between H3 and H5 at 7.29 ppm with C3 and C5 at 128.74 ppm in the noted segment. A similar correlation can also be found on H2′, H6′, H3′ and H5′of the benzyl segment with C2′, C6′, C3′ and C5′ atoms, respectively (Table 4). The H4′ (δ = 7.25 ppm) of the benzyl segment correlates with C4′ at δ = 126.88 ppm.

The 2D ^1H–^{13}C HMBC spectrum (Figure 12) has been used for assignment of the carbon atoms not-bonded to the hydrogen atom in compound **1**. This spectrum shows the connectivities of the proton atoms with ^2J and ^3J relations to carbon atoms. The HMBC spectrum of **1** shows the correlation between the C1′ atom (δ = 138.28 ppm) with CH_2 protons (δ = 4.16 and

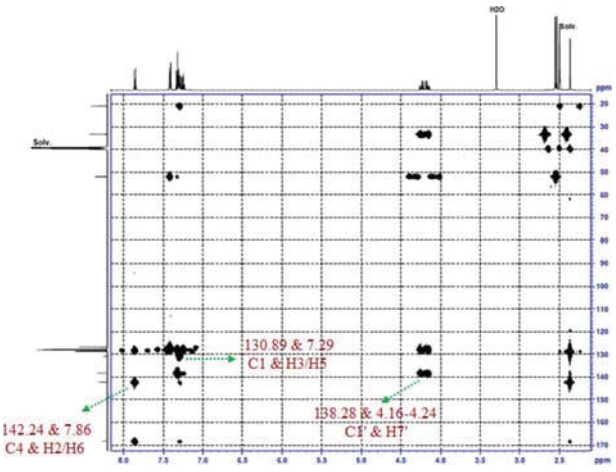

Figure 12. Long range C–H correlation in the HMBC spectrum of **1**.

Table 4. 2D ^{1}H–^{13}C HMQC and HMBC correlations for compounds **1**–**3**.

Atom	HMQC ^{1}J	HMBC ^{2}J	HMBC ^{3}J
1			
H2/H6 ($\delta = 7.86$)	C2/C6 ($\delta = 128.23$)	C3/C5 ($\delta = 128.74$)	C4 ($\delta = 142.24$) C8 ($\delta = 168.31$)
H3/H5 ($\delta = 7.29$)	C3/C5 ($\delta = 128.74$)	C4 ($\delta = 142.24$) C2/C6 ($\delta = 128.23$)	C1 ($\delta = 130.89$) C7 ($\delta = 20.92$)
H7 ($\delta = 2.37$)	C7 ($\delta = 20.92$)	C4 ($\delta = 142.24$)	C3/C5 ($\delta = 128.74$)
H2′/H6′ ($\delta = 7.41$)	C2′/C6′ ($\delta = 127.88$)	C3′/C5′ ($\delta = 128.16$)	C4′ ($\delta = 126.88$)
H3′/H5′ ($\delta = 7.32$)	C3′/C5′ ($\delta = 128.16$)	C2′/C6′ ($\delta = 127.88$)	C1′ ($\delta = 138.28$)
H4′ ($\delta = 7.25$)	C4′ ($\delta = 126.88$)	C3′/C5′ ($\delta = 128.16$)	C2′/C6′ ($\delta = 127.88$)
H7′ ($\delta = 4.16, 4.24$)	C7′ ($\delta = 51.99$)	C1′ ($\delta = 138.28$)	C8′ ($\delta = 33.37$) C2′/C6′ ($\delta = 127.88$)
H8′ ($\delta = 2.54$)	C8′ ($\delta = 33.37$)	—	C7′ ($\delta = 51.99$)
2			
H2/H6 ($\delta = 7.78$)	C2/C6 ($\delta = 128.05$)	C3/C5 ($\delta = 128.68$) —	C4 ($\delta = 141.91$) C8 ($\delta = 167.81$)
H3/H5 ($\delta = 7.26$)	C3/C5 ($\delta = 128.68$)	C4 ($\delta = 141.91$) C2/C6 ($\delta = 128.05$)	C1 ($\delta = 131.28$) C7 ($\delta = 20.88$)
H7 ($\delta = 2.35$)	C7 ($\delta = 20.88$)	C4 ($\delta = 141.91$)	C3/C5 (128.68)
H1′ ($\delta = 3.31$)	C1′ ($\delta = 54.13$)	—	—
3			
H2/H6 ($\delta = 7.80$)	C2/C6 ($\delta = 128.07$)	C3/C5 ($\delta = 128.70$)	C4 ($\delta = 141.96$) C8 ($\delta = 167.82$)
H3/H5 ($\delta = 7.26$)	C3/C5 ($\delta = 128.70$)	C2/C6 ($\delta = 128.07$)	C1 ($\delta = 131.22$) C7 ($\delta = 20.88$)
H1′ ($\delta = 3.07$)	C1′ ($\delta = 38.78$)	C2′ ($\delta = 13.77$)	—
H7 ($\delta = 2.35$)	C7 ($\delta = 20.88$)	C4 ($\delta = 141.96$)	C3/C5 ($\delta = 128.70$)
H2′ ($\delta = 1.04$)	C2′ ($\delta = 13.77$)	C1′ ($\delta = 38.78$)	—

For the numbering of H and C atoms in NMR assignments:

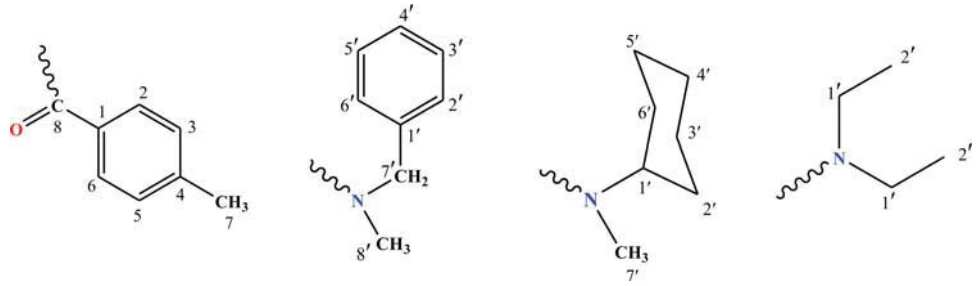

4.24 ppm) with a ^{2}J connectivity. Furthermore, the C1 and C4 atoms of the tolyl segment are respectively correlated with the H3/H5 and H2/H6 atoms with ^{3}J connectivities (Table 4).

Conclusion

A series of three phosphoric triamide analogues were synthesized and crystal structure analysis was used to study the supramolecular behavior of these molecules. From the crystal packing features, it was noted that even though the basic arrangements based on classical NH···O hydrogen bonding are distinctly similar, upon different substitution, the weak intermolecular CH···O interactions assist to construct different superstructures. The intermolecular interactions of these structures were also described by means of Hirshfeld surface analysis. It was also deduced that the H···H, O···H/H···O and C···H/H···C interactions, which are significantly dispersed within the crystal structures, could also be influential factors related to the supramolecular assemblies formed. Having analyzed all the possible intermolecular interactions of these phosphoric triamide analogues, this analysis contributes to explain how this class of molecules with different substitution on the C(O)NHP(O) backbone could possibly be considered for the potential design of new supramolecular compounds.

Experimental

Materials and methods

N-Methylbenzylamine, N-methylcyclohexylamine, diethylamine, 4-methylbenzamide, phosphorus pentachloride, phosphorus pentoxide, acetonitrile and methanol were commercially available and used as received. Chloroform was dried with P_2O_5 and distilled prior to use.

IR spectra for compounds **1**–**3** were recorded using a Buck 500 scientific spectrometer by means of KBr pellets. ^{1}H, ^{13}C and ^{31}P NMR spectra were recorded on Bruker Avance 300 and Bruker Avance III 500 spectrometers. ^{1}H, ^{13}C and ^{31}P chemical shifts were determined relative to TMS and 85% H_3PO_4, respectively, as an internal or external standard. The mass spectra were recorded with an MS model CH7A Varian (EI, 70 eV) spectrometer. High-resolution mass spectra were recorded on a Bruker FTMS 4.7 T BioAPEX II spectrometer. The melting points

of compounds **1**–**3** were also measured by Thermo Scientific IA-9300 apparatus.

X-ray measurements and Hirshfeld surface analysis

Data collection processes were performed for the structures **1** and **2** at 173(2) K on an Agilent Gemini-EOS Single Crystal Auto diffractometer with Cu-Kα radiation, solved by the direct methods algorithm of SHELXS97 and refined by SHELXL97.[34] Data for **3** was obtained at 200(2) K using Cu-Kα radiation with a STOE IPDS II diffractometer and with a graphite monochromator. The structure **3** was solved with SUPERFLIP[35] and refined with the SHELXL2014.[36] All hydrogen atoms were included in the refinement at geometrically fixed positions and refined with a riding model. The molecular graphics were generated by MERCURY[37], OLEX[38] and the DIAMOND[39] for Windows program. The Hirshfeld surfaces and related fingerprint plots were generated by the program Crystal Explorer 3.1.[40]

General procedure for the synthesis of compounds 1–3

4-CH_3-$C_6H_4C(O)NHP(O)Cl_2$ was prepared according to the method used for the analogous compound 4-NO_2-$C_6H_4C(O)NHP(O)Cl_2$, by using 4-CH_3-$C_6H_4C(O)NH_2$ instead of 4-NO_2-$C_6H_4C(O)NH_2$.[41] To synthesize compounds **1**–**3**, a solution of 4 mmol amine in dry $CHCl_3$ (5 mL) was added dropwise to a stirred solution of 1 mmol 4-CH_3-$C_6H_4C(O)NHP(O)Cl_2$ in the same solvent (20 mL) at 0 °C. After 4 h, the solvent was removed in vacuum and the solid obtained was washed with H_2O. Single crystals, suitable for X-ray crystallography, were obtained from a mixture of CH_3OH/CH_3CN (3:1) for **1** and $CH_3OH/CHCl_3$ (1:1) for **2** and **3** at room temperature after a few days.

N-(bis(benzyl(methyl)amino)phosphoryl)-4-methylbenzamide (1)

M.p. 170 °C. ESI–MS: 422.19927 (calcd for $C_{24}H_{29}N_3O_2P^+$ 422.19919). $^{31}P\{^1H\}$ NMR (121.49 MHz, DMSO-d_6, 85% H_3PO_4): 14.76 (s). ^1H NMR (500.13 MHz, DMSO-d_6, TMS): 9.37 (very br. *s*, 1H, CONH), 7.86 (apparent *d*, $J = 8.3$ Hz, 2H, H2/6), 7.41 (*dm*, $J = 7.0$ Hz, 4H, H2′/6′), 7.32 (*tm*, $J = 7.2$ Hz, 4H, H3′/5′), 7.29 (apparent *d*, $J = 7.9$ Hz, 2H, H3/5), 7.25 (*tt*, $J = 7.3$, 1.3 Hz, 2H, H4′), 4.24 (*dd*, $^2J_{HH} = 15.2$ Hz, $^3J_{PH} = 9.3$ Hz, 2H, H7′$_a$), 4.16 (*dd*, $^2J_{HH} = 15.2$ Hz, $^3J_{PH} = 8.9$ Hz, 2H, H7′$_b$), 2.54 (*d*, $^3J_{PH} = 10.1$ Hz, 6H, H8′), 2.37 (*s*, 3H, H7). ^{13}C NMR (125.77 MHz, DMSO-d_6, TMS): 168.31 (*d*, $^2J_{PC} = 2.2$ Hz, C8), 142.24 (*s*, C4), 138.28 (*d*, $^3J_{PC} = 4.3$ Hz, C1′), 130.89 (*d*, $^3J_{PC} = 8.8$ Hz, C1), 128.74 (*s*, C3/5), 128.23 (*s*, C2/6), 128.16 (*s*, C3′/5′), 127.88 (*s*, C2′/6′), 126.88 (*s*, C4′), 51.99 (*d*, $^2J_{PC} = 4.5$ Hz, C7′), 33.37 (*d*, $^2J_{PC} = 5.2$ Hz, C8′), 20.92 (*s*, CH_3, C7). IR (KBr, cm^{-1}): 3087, 2931, 1674 (C═O), 1608, 1454, 1353, 1272, 1192, 1110, 1002, 920, 871, 788. MS (70 eV, EI): m/z (%) = 28 (79), 57 (79), 65 (68), 82 (40), 91 (89), 105 (58), 117 (15), 119 (100), 165 (33), 183 (55), 235 (21), 265 (9), 298 (14), 313 (10), 420 (55), 421 (78).

N-(bis(cyclohexyl(methyl)amino)phosphoryl)-4-methylbenzamide (2)

M.p. 165 °C. ESI–MS: 406.26129 (calcd for $C_{22}H_{37}N_3O_2P^+$ 406.26179). $^{31}P\{^1H\}$ NMR (121.49 MHz, DMSO-d_6, 85% H_3PO_4): 13.77 (s). ^1H NMR (500.13 MHz, DMSO-d_6, TMS): 8.89 (br. *s*, 1H, CONH), 7.78 (apparent *d*, $J = 8.2$ Hz, 2H, H2/6), 7.26 (apparent *d*, $J = 8.0$ Hz, 2H, H3/5), 3.31 (*tdt*, $^3J_{HH} = 11.9$, 3.5 Hz, $^3J_{PH} = 9.3$ Hz, 2H, H1′), 2.52 (*d*, $^3J_{PH} = 10.8$ Hz, 6H, H7′), 2.35 (*s*, 3H, H7), 1.74 (*dm*, $J = 10.2$ Hz, 2H, HX′$_{eq}$), 1.72 (*dm*, $J = 10.2$ Hz, 2H, HX′$_{eq}$), 1.62 (*dm*, 2H, HX′$_{eq}$), 1.59 (*dm*, 2H, HX′$_{eq}$), 1.55 (*dm*, 2H, HX′$_{eq}$), 1.50 (*qd*, $J = 12.3$, 3.6 Hz, 2H, HX′$_{ax}$), 1.46 (*qd*, $J = 12.3$, 3.4 Hz, 2H, HX′$_{ax}$), 1.22 (*qt*, $J = 13.1$, 3.6 Hz, 2H, HX′$_{ax}$), 1.18 (*qt*, $J = 13.1$, 3.5 Hz, 2H, HX′$_{ax}$), 1.02 (*qt*, $J = 12.9$, 3.5 Hz, 2H, H4′$_{ax}$). ^{13}C NMR (125.77 MHz, DMSO-d_6, TMS): 167.81 (*d*, $^2J_{PC} = 2.2$ Hz, C8), 141.91 (*s*, C4), 131.28 (*d*, $^3J_{PC} = 8.9$ Hz, C1), 128.68 (*s*, C3/5), 128.05 (*s*, C2/6), 54.13 (*d*, $^2J_{PC} = 4.7$ Hz, C1′), 30.36 (*d*, $^3J_{PC} = 3.5$ Hz, C6′ or 2′), 30.18 (*d*, $^3J_{PC} = 2.0$ Hz, C2′ or 6′), 27.52 (*d*, $^2J_{PC} = 5.0$ Hz, C7′), 25.67 (*s*, C5′ or 3′), 25.63 (*s*, C3′ or 5′), 25.07 (*s*, C4′), 20.88 (*s*, CH_3, C7). IR (KBr, cm^{-1}): 3077, 2933, 2856, 1671 (C═O), 1611, 1448, 1271, 1221, 1185, 1162, 1106, 1005, 978, 878, 821. MS (70 eV, EI): m/z (%) = 28 (72), 42 (42), 57 (63), 70 (72), 83 (40), 91 (63), 98 (36), 112 (100), 117 (40), 119 (66), 158 (32), 175 (28), 243 (30), 285 (22), 290 (44), 320 (10), 404 (62), 405 (68), 407 (35).

N-(bis(diethylamino)phosphoryl)-4-methylbenzamide (3)

M.p. 147 °C. ESI–MS: 326.19893 (calcd for $C_{16}H_{29}N_3O_2P^+$ 326.19919). $^{31}P\{^1H\}$ NMR (121.49 MHz, DMSO-d_6, 85% H_3PO_4): 13.09 (s). ^1H NMR (500.13 MHz, DMSO-d_6, TMS): 8.98 (very br. *s*, 1H, CONH), 7.80 (apparent *d*, $J = 8.2$ Hz, 2H, H2/6), 7.26 (apparent *d*, $J = 7.9$ Hz, 2H, H3/5), 3.07 (*dq*, $^3J_{PH} = 11.1$ Hz, $^3J_{HH} = 7.1$ Hz, 8H, H1′), 2.35 (*s*, 3H, H7), 1.04 (*t*, $J = 7.1$ Hz, 12H, H2′). ^{13}C NMR (125.77 MHz, DMSO-d_6, TMS): 167.82 (*d*, $^2J_{PC} = 2.1$ Hz, C8), 141.96 (*s*, C4), 131.22 (*d*, $^3J_{PC} = 8.6$ Hz, C1), 128.70 (*s*, C3/5), 128.07 (*s*, C2/6), 38.78 (*d*, $^2J_{PC} = 4.9$ Hz, C1′), 20.88 (*s*, CH_3, C7), 13.77 (*d*, $^3J_{PC} = 2.5$ Hz, C2′). IR (KBr, cm^{-1}): 3068, 2968, 2878, 2740, 1672 (C═O), 1611, 1514, 1462, 1382, 1277, 1214, 1174, 1111, 1061, 1028, 947, 867, 820, 746, 718, 645. MS (70 eV, EI): m/z (%) = 28 (100), 43 (88), 64 (88), 72 (93), 83 (41), 96 (43), 117 (40), 119 (71), 127 (88), 148 (65), 159 (59), 166 (23), 191 (24), 253 (88), 277 (11), 322 (88), 324 (88), 325 (3).

Acknowledgments

Support of this investigation by Ferdowsi University of Mashhad (Project No. 3/28386) is gratefully acknowledged. Jerry P. Jasinski acknowledges the NSF-MRI program (grant No. CHE-1039027) for funds to purchase the X-ray diffractometer to perform the crystallography experiments of structures **1** and **2**. For structure **3**, the X-ray crystallography experiment was supported by FriMat, University of Fribourg.

Supplementary data

CCDC 1045700, 1030528 and 1030678 contain the supplementary crystallographic data for **1, 2** and **3**. These data can be obtained free of charge via http://www.ccdc.cam.ac.uk/conts/retrieving.html, or from the Cambridge Crystallographic Data Centre, 12 Union Road, Cambridge CB2 1EZ, UK; fax: (+44) 1223-336-033, or e-mail: deposit@ccdc.cam.ac.uk.

ORCID

Mehrdad Pourayoubi http://orcid.org/0000-0001-5608-2111

References

[1] Biradha, K. *CrystEngComm* **2003**, *5*, 374-384.
[2] Aakeröy, C. B.; Champness, N. R.; Janiak, C. *CrystEngComm* **2010**, *12*, 22-43.
[3] Desiraju, G. R. *Nat. Mater.* **2002**, *1*, 77-79.
[4] Sharma, C. V. K. *Cryst. Growth Des.* **2002**, *2*, 465-474.
[5] Desiraju, G. R. *Mater. Sci.* **1997**, *2*, 451-454.
[6] Hudson, H. R.; Czugler, M.; Lee, R. J.; Woodroffe, T. M. *Phosphorus Sulfur Silicon Relat. Elem.* **2016**, *191*, 469-477.
[7] Kunda, U. M. R.; Yamada, M.; Hamada, F. *Phosphorus Sulfur Silicon Relat. Elem.* **2017**, *192*, 276-282.
[8] Thaimattam, R.; Reddy, D. S.; Xue, F.; Mak, T. C. W.; Nangia, A.; Desiraju, G. R. *J. Chem. Soc., Perkin Trans. 2* **1998**, 1783-1790.
[9] Kojić-Prodić, B.; Štefanić, Z.; Žinić, M. *Croat. Chem. Acta* **2004**, *77*, 415-425.
[10] Głowacki, E. D.; Irimia-Vladu, M.; Bauer, S.; Sariciftci, N. S. *J. Mater. Chem. B* **2013**, *1*, 3742-3753.
[11] Thakur, T. S.; Dubey, R.; Desiraju, G. R. *IUCrJ* **2015**, *2*, 159-160.
[12] Roman, M.; Cannizzo, C.; Pinault, T.; Isare, B.; Andrioletti, B.; van der Schoot, P.; Bouteiller, L. *J. Am. Chem. Soc.* **2010**, *132*, 16818-16824.
[13] Ravat, P.; Seetha Lekshmi, S.; Biswas, S. N.; Nandy, P.; Varughese, S. *Cryst. Growth Des.* **2015**, *15*, 2389-2401.
[14] Steiner, T. *Angew. Chem. Int. Ed.* **2002**, *41*, 48-76.
[15] Samipillai, M.; Bhatt, N.; Kruger, H. G.; Govender, T.; Naicker, T. *J. Mol. Struct.* **2016**, *1122*, 37-47.
[16] Bosch, E. *Acta Cryst. C* **2016**, *72*, 748-752.
[17] Nogueira, T. C. M.; Pinheiro, A. C.; Wardell, J. L.; de Souza, M. V. N.; Abberley, J. P.; Harrison, W. T. A. *Acta Cryst. C* **2015**, *71*, 647-652.
[18] Desiraju, G. R. *Chem. Commun.* **2005**, 2995-3001.
[19] Wahl, M. C.; Sundaralingam, M. *Trends in Biol. Sci.* **1997**, *22*, 97-102.
[20] Doskocz, M.; Gancarz, R. *Phosphorus Sulfur Silicon Relat. Elem.* **2009**, *184*, 1363-1373.
[21] Pourayoubi, M.; Rostami Chaijan, M.; Padelková, Z.; Ružicka, A. *Phosphorus Sulfur Silicon Relat. Elem.* **2013**, *188*, 224-231.
[22] Pourayoubi, M.; Toghraee, M.; Zhu, J.; Dušek, M.; Bereciartua, P. J.; Eigner, V. *CrystEngComm* **2014**, *16*, 10870-10887.
[23] Yang, L.; Powell, D. R.; Houser, R. P. *Dalton Trans* **2007**, 955-964.
[24] Keikha, M.; Pourayoubi, M.; Tarahhomi, A.; van der Lee, A. *Acta Cryst. C* **2016**, *72*, 251-259.
[25] Pourayoubi, M.; Tarahhomi, A.; Saneei, A.; Rheingold, A. L.; Golen, J. A. *Acta Cryst. C* **2011**, *67*, 265-272.
[26] Corbridge, D. E. C. *Phosphorus, an Outline of its Chemistry, Biochemistry and Technology*, 5th ed., New York: Elsevier Science, **1995**.
[27] Spackman, M. A.; Byrom, P. G. *Chem. Phys. Lett.* **1997**, *267*, 215-220.
[28] Hirshfeld, F. L. *Theor. Chim. Acta* **1977**, *44*, 129-138.
[29] McKinnon, J. J.; Spackman, M. A.; Mitchell, A. S. *Acta Cryst. B* **2004**, *60*, 627-668.
[30] Spackman, M. A.; Jayatilaka, D. *CrystEngComm* **2009**, *11*, 19-32.
[31] Spackman, M. A.; McKinnon, J. J. *CrystEngComm* **2002**, *4*, 378-392.
[32] Mizrahi, V.; Modro, T. A. *J. Org. Chem.* **1982**, *47*, 3533-3539.
[33] Gholivand, K.; Madani Alizadehgan, A.; Mojahed, F.; Soleimani, P. *Polyhedron* **2008**, *27*, 1639-1649.
[34] Sheldrick, G. M. *Acta Cryst. A* **2008**, *68*, 112-122.
[35] Palatinus, L.; Chapuis, G. *J. Appl. Cryst.* **2007**, *40*, 786-790.
[36] Sheldrick, G. M. *Acta Cryst. C* **2015**, *71*, 3-8.
[37] Macrae, C. F.; Bruno, I. J.; Chisholm, J. A.; Edgington, P. R.; McCabe, P.; Pidcock, E.; Rodriguez-Monge, L.; Taylor, R.; van de Streek, J.; Wood, P. A. *J. Appl. Cryst.* **2008**, *41*, 466-470.
[38] Dolomanov, O. V.; Bourhis, L. J.; Gildea, R. J.; Howard, J. A. K.; Puschmann, H. OLEX2: A complete structure solution, refinement and analysis program. *J. Appl. Cryst.* **2009**, *42*, 339-341.
[39] Brandenburg, K.; Putz, H. *DIAMOND Crystal Impact*; Germany: GbR Bonn, **1999**.
[40] Wolff, S. K.; Grimwood, D. J.; McKinnon, J. J.; Turner, M. J.; Jayatilaka, D.; Spackman, M. A. *Crystal Explorer, University of Western Australia*, Australia, **2013**.
[41] Pourayoubi, M.; Sabbaghi, F. *J. Chem. Cryst.* **2009**, *39*, 874-880.